

AD-A210 511

FTD-ID(RS)T-0639-34

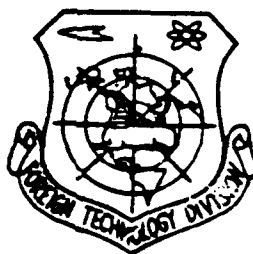
## FOREIGN TECHNOLOGY DIVISION



THE STEADY STATE BURNING MECHANISM OF COMPOSITE SOLID  
PROPELLANTS INCLUDING THOSE WITH NEGATIVE  
PRESSURE EXPONENTS

by

X. Wengan, L. Baoxuan, W. Kexiu



DTIC  
JUL 26 1989  
9E D

Approved for public release;  
distribution unlimited.

89 . 7 26 062

## EDITED TRANSLATION

FTD-ID(RS)T-0639-84

21 June 1984

MICROFICHE NR: FTD-84-C-000617

THE STEADY STATE BURNING MECHANISM OF COMPOSITE  
SOLID PROPELLANTS INCLUDING THOSE WITH NEGATIVE  
PRESSURE EXPONENTS

By: X. Wengan, L. Baoxuan, W. Kexiu

English pages: 44

Source: Yuhang Xuebao, Nr. 3, 1983, pp. 1-19

Country of origin: China

Translated by: SCITRAN

F33657-81-D-0263

Requester: FTD/TQTA

Approved for public release; distribution unlimited.

THIS TRANSLATION IS A RENDITION OF THE ORIGINAL FOREIGN TEXT WITHOUT ANY ANALYTICAL OR EDITORIAL COMMENT. STATEMENTS OR THEORIES ADVOCATED OR IMPLIED ARE THOSE OF THE SOURCE AND DO NOT NECESSARILY REFLECT THE POSITION OR OPINION OF THE FOREIGN TECHNOLOGY DIVISION.

PREPARED BY:

TRANSLATION DIVISION  
FOREIGN TECHNOLOGY DIVISION  
WP.AFB, OHIO.

FTD -ID(RS)T-0639-84

Date 21 Jun 19 84

## **DISCLAIMER NOTICE**

**THIS DOCUMENT IS BEST QUALITY  
PRACTICABLE. THE COPY FURNISHED  
TO DTIC CONTAINED A SIGNIFICANT  
NUMBER OF PAGES WHICH DO NOT  
REPRODUCE LEGIBLY.**

The Steady State Burning Mechanism of Composite Solid  
Propellants Including those with Negative Pressure Exponents

Xu Wengan    Li Baoxuan    Wang Kexiu

ABSTRACT

In order to study the steady state burning mechanism of AP-based composite solid propellants including those with negative pressure exponents, we applied the scanning electron microscope to examine samples of extinguished combustion strands and we also applied the single-frame microphotography of self-illumination or laser-shadow to observe the burning samples. We found that the covering of the molten binder over the AP surface was not a particular phenomenon of the PU propellant in the "mesa" burning area, but rather a general phenomenon taken place over an extensive region. We showed indication that local covering may not have resulted in local extinction and we further proposed a new theoretical model which takes into consideration the combined effect of the converging of the molten binder on the AP surface and the existence of condensed phase reaction as well as the reversed

# GRAPHICS DISCLAIMER

All figures, graphics, tables, equations, etc. merged into this translation were extracted from the best quality copy available.

Accession For	
NTIS GPOSI	<input checked="" type="checkbox"/>
DTIC TAB	<input checked="" type="checkbox"/>
Unannounced	<input type="checkbox"/>
Justification	
By	
Distribution Code	
Availability Codes	
Avail and/or	
Dist	Special
A-123	



gasification under the surface covering. This model can be used for AP-based solid composite propellants which include the easily melted binder. This model exhibits the capability of explaining the "plateau", "mesa", and normal burning behavior and it can also be used to analyze the effects of initial temperature and the AP particle size on the burning characteristics. Furthermore, this model can serve as a basis for studying the erosive combustion and non-steady state combustion of propellants which include the "mesa" propellants.

*Research on Solid Rocket Propellants, Erosive Combustion, Non-Steady State Combustion, Transitions, China Science Library*

## I. INTRODUCTION

The composite solid propellants usually have two basic types of burning models; one is the gas phase type and the other is the condensed phase type. Among these models the "GDF" model is representative of the gas phase models and the "BDP" is representative of the condensed phase models. (It should be noted that in the early 1960's scientists in our country, such as comrades Zhang Cun Hao, He Guo Zhong, and Yang Pei Qing, have proposed a complete multiple layer flame model which can be guided and implemented<sup>[1]</sup>. Some of the mathematical treatments used by this paper are developed in light of their results. In recent years, based on the foundation of these

two types of basic models mentioned above, scientists made the breakthrough of the limitation of single mode single dispersion of oxidation reagent particles and introduced statistical methods more fully into this problem, which has a strong degree of randomness. One especially clear example is the establishment of the contemporary models such as the "PEM" model which can analyze the problem more fully under more realistic conditions. Unfortunately none of the models can be used to explain the "plateau" and "mesa" effects.

J.H. Robert<sup>[2]</sup> has proposed the combustion speed relation equation  $r = a p^{\log(1/Le)}$  as early as 1966. This was actually a relatively abstract model for steady state burning. Even though this was only a hypothesis of his, it represents a bold attempt to come up with a model which attempts to explain all the combustion speed characteristics of normal, "plateau", and "mesa" burning fully. This author believes that these combustion speed characteristics are only manifestations of a single unified burning problem under different conditions. This is why when we are studying the individual mechanism of the various characteristic areas, we should also consider the internal connection among these various characteristic areas so we can more deeply explore the nature of the problem. We can only tackle the problem associated with a unified burning

mechanism which varies with conditions when we can propose a complete theoretical model which can provide a full explanation of all the burning characteristics of the composite solid propellants. This is the objective of this study and we start by exploring the nature of the "mesa" effect. We also endeavor to propose a unified model.

---

This paper was received on April 17, 1982.

The so called "mesa" effect indicates that the combustion speed of the solid propellant exhibits a negative exponent relationship with the pressure and this burning phenomenon was discovered in the 1950's or even earlier. There has been no in-depth study into this effect up to this date, since it has not received the proper application attention it deserved in the past. At present, however, an in-depth study into this effect appear, quite necessary since it provides a probable path for the study of the adjustment of the impulse power of a solid rocket propeller [3] as well as the adjustment of the flow volume of the solid combustion gas generator [4]. Even though we have not seen an analytical model which describes this effect up to date, there have been numerous experimental observations and valuable descriptions about the mechanisms that can serve as basis for our study. (The relevant references are in [5] - [13]). This study starts from phenomena observed



during the experiments. We consider primarily viewpoints expressed by M. Summerfield<sup>[3]</sup>, D.B. Spalding<sup>[5]</sup>, and C. Guirao<sup>[14]</sup> and then propose a model based on the "BDP" model. Our model attempts to fully describe the "plateau", "mesa", and normal burning behavior.

#### EXPLANATION OF SYMBOLS

- A the factor in front of the exponent in the Arrhenius Equation
- $B_1, B_2, B_3$  proportionality constants in the corresponding relationship equations
- $C_p$  specific heat under constant pressure
- $D_0$  standard dispersion coefficient under reference pressure
- $d$  statistically averaged diameter of the AP particle
- $E_f$  activation energy associated with the thermal dissociation of the binder
- $E_{ox}$  activation energy associated with the interface reaction of the oxidation reagent
- G fractional mass of the AP that was used up during the condensed phase reaction
- h the thickness of the liquid layer covered by the binder or the difference in height between the oxidation reagent and the surface of the binder which was reflected in the equation representing  $S_{ox}/S_0$

$K$  speed constants associated with the various chemical reactions  
 $K_0$  parameter of ignition delay associated with the oxidation reagent  
 $Le \equiv \frac{\lambda}{\rho C_p D}$  , Lewis number  
 $\dot{m}$  mass flow rate  
 $n$  orders of reaction of the various chemical reaction  
 $P$  pressure  
 $Q$  reaction heat associated with a unit mass of the reagent  
 $Q_0$  reaction heat of dispersed flame in area I associated with a unit mass  
 $Q_R$  reaction heat of mixed flame in area I per unit mass  
 $Q_F$  reaction heat for the dissociation of a unit mass of the binder  
 $Q_L$  condensed phase reaction heat for a unit mass of AP  
 $Q_S$  interface reaction heat for a unit mass of AP  
 $q$  evaporation heat for a unit mass of AP  
 $R^0$  universal gas constant  
 $S_0$  the total surface area of the oxidation reagent and binder in area II  
 $T$  temperature or the characteristic temperature corresponding to the dispersed flame  
 $T_0$  initial temperature of the propellant  
 $T_f$  the adiabatic flame temperature of the propellant and the temperature of the burning gas

$t_{ign}$  time of delayed ignition for the oxidation reagents  
 $M$  gm molecular weight  
 $M_g$  gm molecular weight of the gaseous product of the AP condensed phase reaction  
 $X$  transmission distance from the burning surface corresponding to the various reactions in area II  
 $Y$  transmission distance from the AP surface corresponding to the various reactions in area I  
 $a$  fractional mass of the oxidation reagent in the propellant  
 $\beta_F$  the fraction of the reagent that enters the initial flame  
 $\gamma$  the fractional area of the surface of the oxidation reagent that is being covered by the melten binder  
 $\xi$  the fractional volume of the oxidation reagent  
 $\lambda$  coefficient of thermal conductivity  
 $\rho$  density  
 $\rho_s$  density of the solid propellant  
 $\xi''$  the dimensionless transmission distance corresponding to the various reactions  
 superscript  
 I the corresponding parameter in area I where the oxidation reagent is being covered by the binder  
 II the corresponding parameter in area II where the oxidation reagent is not being covered  
 subscript  
 AP parameter corresponding to AP

$AP_{(g)}$  parameter corresponding to the AP vapor  
 D parameter corresponding to the expansion process  
 FF parameter corresponding to the final flame in area II  
 f parameter corresponding to the binder  
 g parameter corresponding to the gaseous state  
 ox parameter corresponding to the oxidation reagent  
 PF parameter corresponding to the initial flame in area II  
 S parameters corresponding to the AP surface in area I or  
 burning surface in area II  
 2 parameter corresponding to the premixed flame in area I  
 3 parameter corresponding to the expansion flame in area I  
 I parameter corresponding to area I  
 II parameter corresponding to area II

## II. EXPERIMENTAL RESULTS AND ANALYSIS

### (I) General Conditions:

The types of propellants used in the experiments and their combustion speeds are shown in Table 1.

In order to observe and verify the condition of the covering of the binder on the AP surface, we connected one end of a "T" shaped generator to a microsecond class interruption opening mechanism, and applied the method of rapid reducing pressure

extinction to obtained extincted samples under different pressure. During the interruption process we have not used any gas or liquid to aid the process of extinction. According to the criteria provided by references [15], [16] we can deduce that the samples we have obtained all retained their true conditions on the burning surface prior to the interruption and there was no destruction due to the "second flame". This judgement was verified by the consistency of the photographs taken by the scanning electron microscope on the burning sample with the interrupted sample. The regularity of the surface structure as observed by the scanning electron microscope also verified this point.

1. 表：推进剂类型及燃速

2. 压 力 (kg/cm <sup>2</sup> )	3. 燃 速 (mm/sec)	
	4. 含铝PU-AP型(S <sub>04-5</sub> )	5. 不含铝PU-AP型(S <sub>04-5A</sub> )
10		2.79
20		3.61
25		3.75
30	3.97	3.62
35		3.35
40	3.98	3.19
45		中途自熄火
50	3.85	中途自熄火
60	3.65	
70	3.51	

1. Table 1 Types of propellants and their combustion speed.

2. pressure      3. combustion speed      4. PU-AP type(S<sub>04-5</sub>) which contains aluminum      5. PU-AP type (S<sub>04-5A</sub>) which contains no aluminum

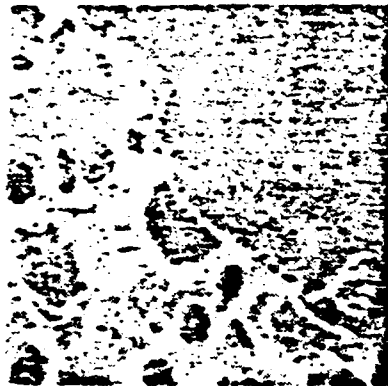
In order to facilitate the observation of the relationship of relative position between the binder and AP on the burning surface, we have very carefully soaked a portion of the extinguished samples one by one in water for about 5 minutes so the AP on the surface could be dissolved and only the framework of the binder would remain. The samples after extinction (including those soaked in water and then oven dried) were then placed under a S4-10 type and a S600 type scanning electron microscope ("SEM") to conduct analytical photography on the burning surface and the cross-section. These samples were also examined using regular microscopes. At the same time we have also conducted single-frame microphotography of flame self-illumination or laser-shadow to observe the samples in the combustion process through the transparent window of the combustion chamber.

## (II) Experimental Results:

1. From the SEM photographs, we can see that the burning surfaces of almost all the samples have melted binder covering the surface of the AP crystal (as shown in Figures 1, 4, 5). The self-illumination photography also indicates that, under low pressure in the non "mesa" area and high pressure in the "mesa" area, the mobility of the binder was extremely good. The

binder in the area ignited first would even flow to the surface that had not been ignited where it formed a cold condensed bulge due to the coldness it encountered (Figure 2).

---



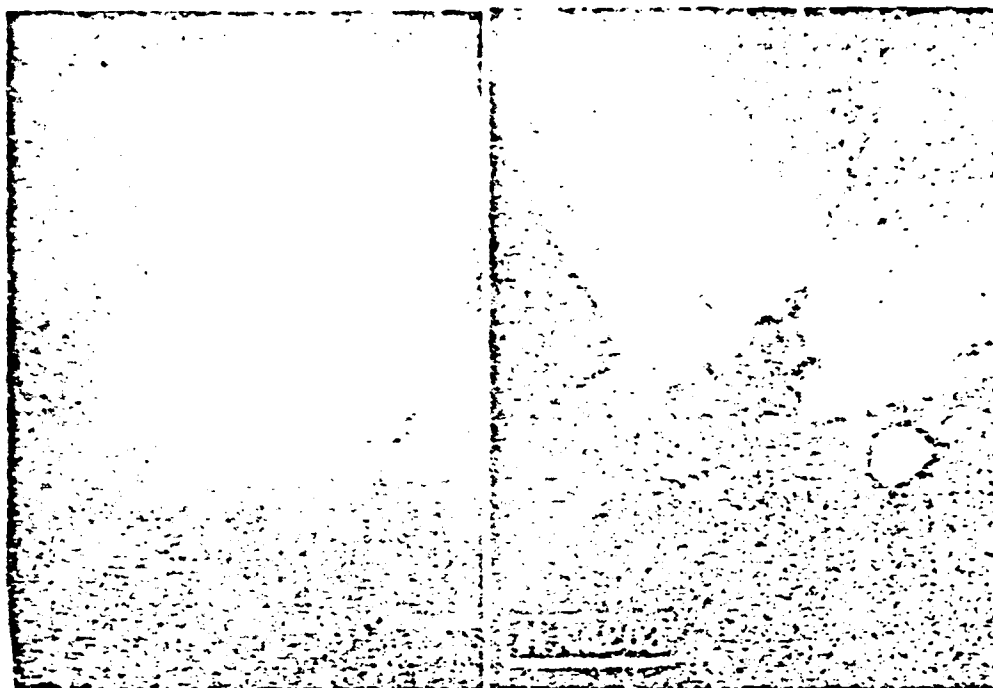
S04-5A  $P=38.5\text{kg/cm}^2$  100x (水泡侧视) 1.



S04-5A  $P=38.5\text{kg/cm}^2$  2K (水泡侧视) 2.

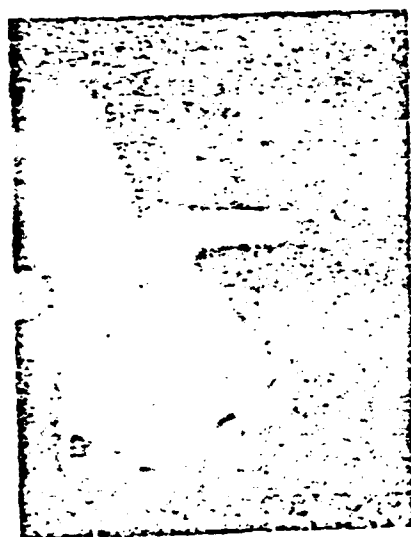
3. 图1 粘合剂复盖层及其侧视图

1. (cross-sectional view of the water soaked sample)
  2. (cross-sectional view of the water soaked sample)
  3. Figure 1 The covering layer of the binder and its cross-sectional view.
-

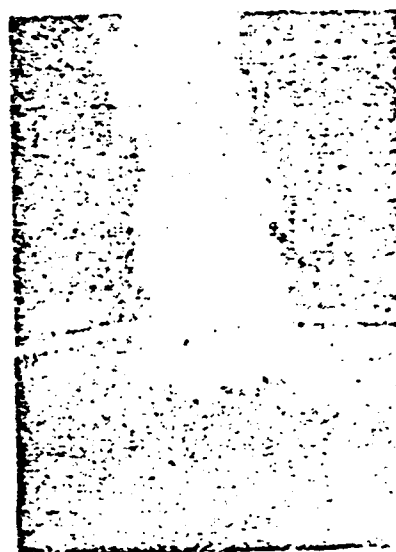


S04-5 PU-AP-Al  $P=15\text{kg/cm}^2$

46-1 CTPB-AP-Al  $P=22\text{kg/cm}^2$



S04-5A PU-AP  $P=24\text{kg/cm}^2$

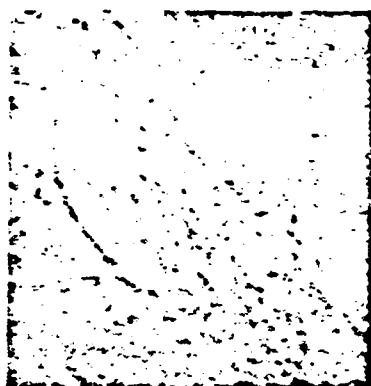


S04-5 PU-AP-Al  $P=32.5\text{kg/cm}^2$

1. 图2 反映了粘合剂流动的自发光照片

1. Figure 2 The self-illumination photographs that reflect the mobility of the binder





S04-3A  $P=38.5\text{ g/cm}^3$  220x (正观) 1.



S04-5A  $P=42.9\text{ kg/cm}^3$  200x (正观) 2.

S04-5A (No.58195)  $P=42.9\text{ kg/cm}^3$  1K (正观) 3.

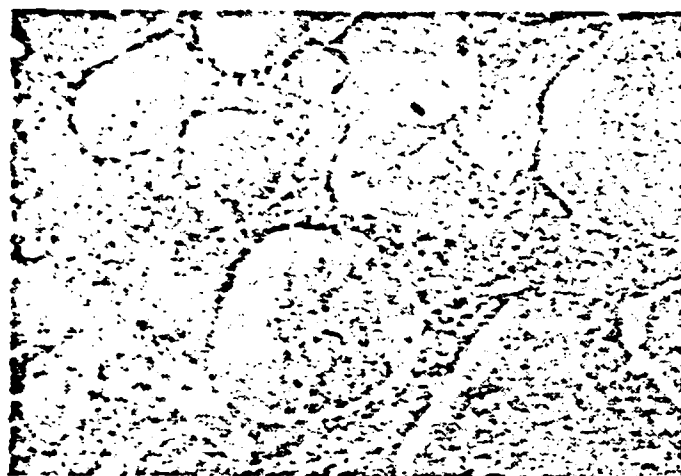
4. 图3 AP颗粒被局部复盖的典型情况

1. (cross-sectional view) 2. (top view) 3. (top view)

4. Figure 3 The typical situation where the AP particles are partially being covered.

2. Observations of the top view and side view of the images of the burning surfaces are shown in Figure 3. The surface of the large oxidation reagent particles was covered by the binder and it formed a straw hat shape. The edge of the hat was the binder which covered the oxidation reagents and the central portion was the volcano crater shaped or cauliflower shaped surface of the oxidation reagent which protruded out relative to its surrounding.

3. There were regular differences between the burning surfaces of the samples extinguished under different pressures. This was especially clear for the S04-5A prescription where there clearly existed different covering areas by the binder on the surfaces of the large oxidation reagent particles (Figure 4). It can also be seen that in the obvious "mesa" area the covered area appears more extensive with higher pressure, while in the non "mesa" area (or its vicinity) there was also a considerable area under low pressure. The S04-5 prescription which contains aluminum also shows this regularity.



S04-5A  
 $P = 23.6 \text{ kg/cm}^2$   
 160X  
 1. (正观)



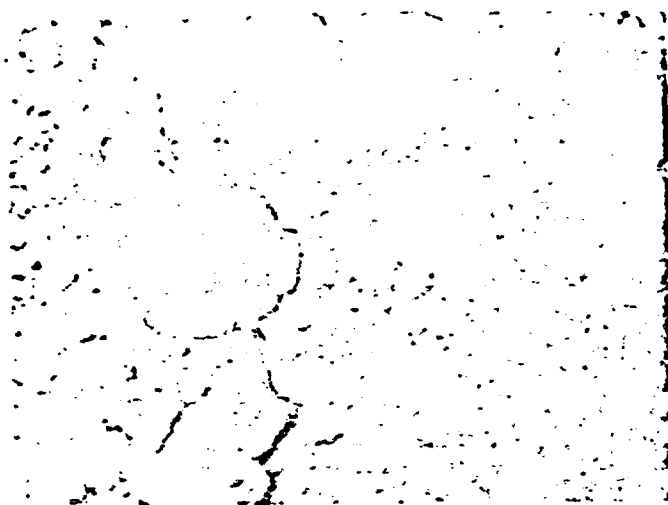
S04-5A  
 $P = 32.0 \text{ kg/cm}^2$   
 160X  
 2. (正观)



S04-5A  
 $P = 38.5 \text{ kg/cm}^2$   
 160X  
 3. (正观)

4. 图：压力对粘料覆盖情况的影响

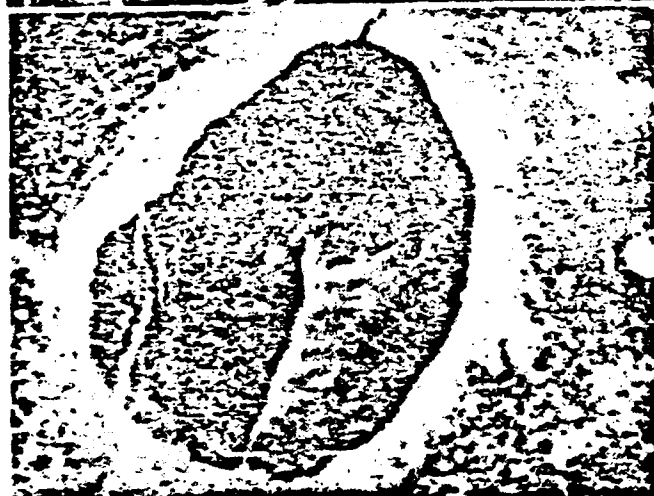
1. (top view)    2. (top view)    3. (top view)  
 4. Figure 4 The effect of pressure on the covering condition  
 of the binder.



S04-5A  
 $P = 38.5 \text{ kg/cm}^2$   
 640×  
 1. (水泡、正视)



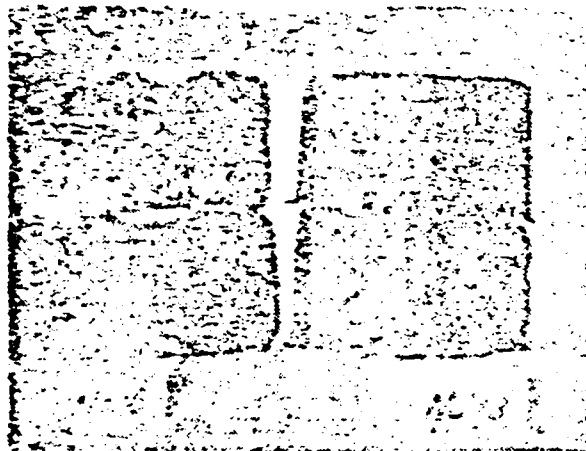
S04-5A  
 $P = 38.5 \text{ kg/cm}^2$   
 640×  
 2. (水泡、正视)



S04-5A  
 $P = 38.5 \text{ kg/cm}^2$   
 640×  
 3. (水泡、正视)

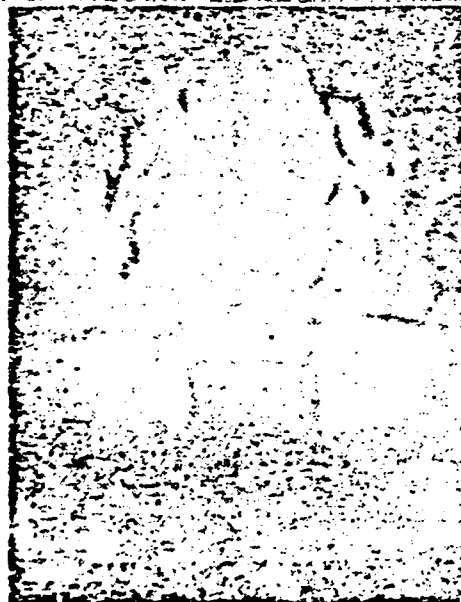
4. 图5 融合剂时 AP 表面复盖的不同情况

1. (water soaked, top view)
2. (water soaked, top view)
3. (water soaked, top view)
4. Figure 5 Different covering conditions of the binder on the AP surface.



No. 16      No. 18  
S04-5A      S04-5A  
 $P = 32 \text{ kg/cm}^2$     $P = 38.5 \text{ kg/cm}^2$

1. 炮火药环的外观  
(1:1)



S04-5A  
 $P = 23.8 \text{ kg/cm}^2$   
2. 激光阴影  
(~7:1)

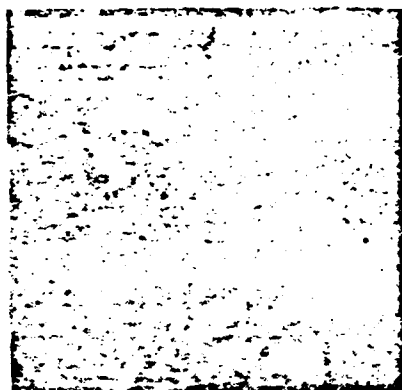
3. 图6 壳状凹坑的形状

1. the exterior appearance of the propellant ring
2. laser shadow
3. Figure 6 The concave shaped crater which looks like the "shell crater".

4. The different conditions of the AP surface covered by the binder under the same pressure (Figure 5) indicate that the covering of each AP particle by the binder could have variation ranging from a local phenomenon to a phenomenon affecting a majority (or all) of the cases. This also means that under a partial covering situation the retreating speed of the covered portion would be smaller than that for the portion that was not covered.

5. The surfaces of a majority of the S04-5A extinguished samples ( in obvious "mesa" area or under the pressure in its vicinity) exhibited concave craters with diameters from 3 to 4 mm which were similar to shallow shell craters. At the same time the laser shadow photographs of this prescription under a pressure of  $24 \text{ kg/cm}^2$ , corresponding to the condition at the intersection of the "mesa" and non "mesa" areas, also show similar "shell craters" (Figure 6).

6. Under the stereoscopic microscope the extinguished samples prepared from the S04-5 prescription show signs of various kinds of "stone forest" shaped small "mountains" standing on top of the burning surface. We can also see some of these features from the SEM photographs (Figure 7).



S04-5  
 $P = 60 \text{ kg/cm}^2$   
 2K

1. 图7 类“石林”状物的“SEM”照片

1. Figure 7 The "SEM" photograph that shows features similar to a "stone forest" shape.

### (III) Experimental Results and Analysis:

Based on the experimental results shown above, the commonly recognized diagnosis [7] - [13] that the "mesa" effect is produced by the local extinction caused by the local covering is questionable. We can say this since in addition to our results reference [9] also mentioned that a prescription with a positive pressure exponent under pressures of 1 - 100 atm would have the burning surface covered with a molten binder layer associated with samples extinguished under all pressures. Derr and Boggs [10] have examined SEM photographs of the extinguished samples of the PU-AP type prescriptions with positive pressure exponents and they have discovered indication that under

relatively high pressure (about  $56.3 \text{ kg/cm}^2$ ) the AP crystal was lying on a shallow concave trough and its surface was covered by the binder. This is almost exactly the same as our result, except that the magnitude of the pressure is different. In addition, the Chinese Technology University has obtained a self-illumination photograph which shows that when a CTPB-AP type prescription with a positive pressure exponent was burning, the molten binder was mobile and the binder encountered coldness on the surface that was not burning and subsequently formed a cold condensed bulge (Figure 2). From the research reports concerning the experiments of double-layered combustion devices [17], [18], we can see that there are widespread melting and flowing phenomenon on top of the AP layer for the CTPB and even HTPB during the combustion period of these doubled-layered devices with conditions close to the realistic combustion process of the propellant. This is why the covering of the AP surface by the molten binder under certain conditions is actually not a particular phenomenon of the PU propellant in the "mesa" area. It is rather a general phenomenon which can take place in a much greater range than the "mesa" area of the PU propellant.



Local covering may not result in local extinction. From the photographs obtained from the single-frame microphotography of the self-illuminating flame (Figure 2), we can see that there was no extinction over a wide area corresponding to a pressure with a wide spread covering ( $24 \text{ kg/cm}^2$ ) for the S04-5A prescription. If we simply think that local covering will lead to local extinction and subsequently produce the "mesa" effect, it will not only be difficult for us to explain the experimental results and reports mentioned above but it will also be difficult for us to explain the phenomenon of non steady state burning of the "plateau" and "mesa" propellants. This is the case since a local extinction will have to cause a decrease in the gain of energy that is supporting the oscillating combustion. This in turn contradicts the existence of the "plateau" and "mesa" propellants as well as the existence of the serious non steady state burning phenomenon.<sup>[19]</sup> (During the "T" type generator experiments we have also obtained a unique self excited oscillation result for the S04-5A propellant under a large area covering pressure of  $P = 23 \text{ kg/cm}^2$  and this result is shown in Figure 4.)

Based on the analysis mentioned above, we believe that covering is only one of the conditions for the production of the "mesa" effect. We also assume that its nature is related

to the abnormal burning in the so called "II characteristic area" associated with the explosion and combustion of pure AP. The reasons are: within the four characteristic areas of the explosion and combustion of AP classified by T.L. Boggs et al.<sup>[20]</sup> according to the relationship between the speed of explosion and combustion and pressure, the existence of a II area where the explosion speed increases with the pressure is definite. Watt and Petersen<sup>[21]</sup> and Friedman<sup>[22]</sup> have also estimated this characteristic area where  $dr/dp < 0$ . In addition, the characteristics of this area<sup>[23]</sup> almost without any exception are exhibited in the "mesa" area of the propellant. The  $dr/dp < 0$  are common, the intermittent and fluctuating micro flame can only be seen in the II area associated with the explosion and combustion of AP, and these phenomena are only seen during the burning of the "mesa" propellant. These phenomena are not seen for the burning of the non "mesa" propellants. The latter has been observed by Barrère<sup>[7]</sup>, Summerfield<sup>[8]</sup> and J. Cohen<sup>[13]</sup>. The burning area of the AP has a maximum retreating area in the II area and there are small "mountains" formed by needle like objects on its surface. Both we and J. Cohen<sup>[13]</sup> observed the shallow "shell crater" shaped maximum retreating area on the burning surface of the "mesa" propellant. As for the "stone forest" shaped object which resembles the needle like objects, we have observed this feature from the stereoscopic

microscope as well as the SEM photographs. This is why the authors do not believe that this is only a coincidence; rather we believe that it is due to the covering of the AP surface by the molten binder and the introduction of some reagent which inhibits the combustion speed. These factors under a certain pressure produce burning conditions similar to the explosion and combustion of pure AP in area II.

What is the nature of the cause of the "II area characteristics" for the burning and explosion of AP? We have not seen any study report which provides a full explanation up to this date. C. Guirao and F.A. Williams<sup>[14]</sup> thought that the increase in pressure will increase the absorption of the gases by the condensed phase and the absorbed gases in turn inhibit the destruction of  $\text{ClO}_4$ . This is why the condensed phase reaction will be reduced with an increase in the pressure and hence the combustion speed also decreases with it. Even though this viewpoint lacks direct experimental basis and a description of the quantitative relationship, it is still convincing as far as the explanation of the problem is concerned. This paper will take this hypothesis, which assumes that the condensed phase reaction is a function of the pressure.

### III PHYSICAL MODEL

The combustion of a composite solid propellant is a complicated physical and chemical problem even if the burning process is in steady state. We not only have to study this problem from the angles of chemical dynamics, the heat conduction, the mass conduction, and the chemical thermodynamics, as well as treating the various characteristics of the mechanically mixed substances from the angle of statistics, but we also have to examine the effects of factors such as the relative position of the binder and the oxidation reagent and the mobility of the binder on the covering of the AP crystal surface by the binder from the angle of ordinary mechanics. Specifically, we not only have to treat the whole flame as combinations of different proportions of pre-mixed flame and diffusion flame based on their influence on the combustion speed, but we also should view the combustion speed problems as combinations of condensed phase process and gas phase process and treat them as combinations of different proportions of the condition where the oxidation reagent is covered by the molten binder and the condition where the oxidation reagent is not covered by the binder. At the same time we should also treat the condensed phase reaction as a function of pressure when the surface of the oxidation reagent is covered by the binder and the abnormal burning process is taking place. Also, when we consider the gasification reaction on the interface of gas

and liquid, we should also take into consideration the existence of the reversed process of gasification - the negative-direction gasification.

Based on the concepts mentioned above, we are proposing the following hypotheses for the mechanism of the steady state burning of the composite solid propellants which include the "mesa" type propellants :

1. Based on the presence or absence of the covering of the oxidation reagent surface by the binder, we can classify the burning surface of the propellant into two areas. The area where the surface of the oxidation reagent is covered by the molten binder is called area I, while the area where the surface of the oxidation reagent is not covered by the molten binder is called area II. These two areas will proceed with their different burning patterns based on the burning conditions. Their relative importance in the overall burning process is determined by a composite parameter  $\gamma$  which represents the fractional area of the oxidation reagent surface which is covered by the binder.

2. For area II where the surface of the oxidation reagent is not covered by the binder, it is quite similar to the "BDP" model and we can neglect the negative-direction gasification. The gasification process without the negative-direction gasification is a procedure which can control the combustion

Speed. It also has three types of flames similar to those of the "BDP" model. The first one is still the AP pre-mixed flame for a unit AP propellant; the second one is a diffusion flame in between the AP dissociated gasification products and the surrounding binder or the heat dissociation product of the binder which covers the AP surface nearby (area I). We will call this the initial flame. The third one is a diffusion flame in between the AP flame product and the heat dissociation product of the binder or the neighboring rich-burning product produced by the combustion process in area I. We will call this the final flame. This hypothesis is based on the observation that the AP crystal also exhibits the characteristics of high in the middle and low on the edge before it is covered (Figure 3), similar to the characteristics observed by Derr and Boggr<sup>[10]</sup> for the propellants with positive pressure exponents. This is why we think we should also have a complicated flame structure and we should also have similar multi-layered flames just like the similarities we observed for the surface features.

The condensed phase ( we can deduce that the AP surface that is not covered should be in melting state before the extinction based on the No. 58195 blow up figure of the central portion of the oxidation reagent particle shown in Figure 3)

will have condensed phase reaction taking place in the interior, which releases heat, and the interfacial reaction with dissociation and evaporation taking place on the surface of the liquid layer. The relationship between the combustion speed and the pressure in this area will certainly give positive exponents similar to those in the "BDP" model.

3. In area I where the surface of the oxidation reagent is covered by the molten binder, we assume that the condensed phase with reverse-direction gasification is the procedure that determines the combustion speed. The oxidation reagent maintains the continuous dissociation and gasification on its interface by taking the heat generated by the feed-back of the gas phase flame and the heat generated by its own condensed phase reaction. The product of gasification and the gaseous product of the condensed phase reaction pass through the binder liquid layer on top of them in the form of dispersed phase and subsequently form gas phase reaction with the dissociation product of the binder in the form of a continuous un-steady pre-mixed flame. Finally, the rich-burning reaction product together with the oxygen-rich product on top of area II form a diffused flame. This area is different from area II; the reverse-direction gasification can not be neglected. This is so since when the surface of the oxidation reagent has already been covered by the molten liquid binder layer, the gasified oxidation reagent

molecules can no longer quickly enter the flame area as in area II even under low pressure. Instead, the molecules will have to go through the liquid binder layer that is covering them. This is why the concentration of the gasified molecules is much higher near the interface of the gasification process than is the case with no covering at all. The gm molecular weight that impinges on a unit interfacial area per unit time also increases significantly. This kind of reverse-direction gasification can reach a quite substantial degree even under relatively low pressures. This is why we assume that the dissociation gasification reaction which takes place under these conditions is a reaction somewhere in between the reaction rate process without the reversed direction and the equilibrium process. Since the reverse-direction gasification intensifies with the increase in pressure, the relationship between combustion speed and pressure will obviously have negative exponents when the pressures are higher than a certain value.

At the same time, both recent observations as well as our results indicate that the molten binder layer always exists on the AP surface when the propellant is burning. When the AP surface that is not covered by the binder burns to the degree where it is lower than the liquid surface of the surrounding binder due to the high retreating speed, the molten



binder can flow into the area and cover it. Since the liquid binder layer is closer to the flame than the AP surface that has caved in, its temperature will not be lower than that on the AP surface, so its flowing in will not alter the condition of the AP surface with its own molten liquid layer. This is why the dissociation gasification at this time is still dissociation evaporation. Also as described above, we will further assume that the AP here exhibits condensed phase reaction similar to that described in reference [14], and this reaction is also a function of the pressure: It will increase with the increase in pressure under low pressures, while it will decrease with the increase in pressure just like the explosion and combustion of AP in "area II" when the pressure exceeds a certain value. This kind of a pattern further intensifies the effect of generating negative pressure exponents by the reverse-direction gasification.

4. The fractional area of the surface of the oxidation reagent that is covered by the molten binder  $\gamma$  is determined by the mobility of the binder, the structure of the burning surface (while the structure in turn depends on the pressure), the content of the aluminum powder, the particulate degree of the oxidation reagent, and the property as well as the quantity of the reagent used to adjust the combustion speed. All these factors are obvious. It should be noted that, however, when

the content of the oxidation reagent is high for a prescription due to the low content of the aluminum power, the  $\gamma$  value will increase since the aluminum power and its condensed chunk will exert less resistance to the flow of the binder. When the content of the oxidation reagent is low since the content of the binder is high, the  $\gamma$  value also increases since this increases the possibility of covering. As for the particulate degree of the oxidation reagent, it is obvious that the larger the particle is the longer the flowing distance of the liquid binder layer will have to be in order to cover the surface completely, so the  $\gamma$  value decreases. We should take into consideration that any factor that can increase  $\gamma$  will have a possibility of making the "mesa" effect occur more easily when the propellant is placed over a certain pressure value. So we can extend the analyses mentioned above and discuss how easy or how difficult it is to have a "mesa" effect. These results are consistent with the reports in references [4], [5], [9].

5. The thickness of the covering liquid layer is a random quantity, but its initial mean value is mainly determined by the mobility of the molten binder layer (which possibly contains aluminum power) and the structure of the burning surface. The flowing tendency which produces the covering phenomenon is primarily determined by the difference in height between the surface of the binder liquid and the AP surface. From the angle of the motion, when a certain value is reached which

is great enough to overcome the flow resistance of the molten binder liquid, the flowing and the covering can be realized. After this point the thickness of this covering liquid layer will gradually decrease according to the burning pattern in area I described above. This is why the mean value of the real thickness of this liquid layer, assuming it covers the entire surface completely, depends on not only the mobility of the molten binder liquid but will also be inversely proportional to the retreating speed of the binder in area I.

#### IV MATHEMATICAL TREATMENT

We will first assume that the gas phase reaction is an even phase reaction that is completed in one step. We can neglect the heat loss, and the influence of thermal radiation, and assume that the particle of the oxidation reagent is spherical and it has a single mode single dispersion. Next, we simplify the multi-dimensional physical model into a one-dimensional model so we can facilitate the mathematical treatment. The areas I and II mentioned above are usually two adjacent areas and there is usually a mass exchange relationship between them since the mixture proportionality is different. Based on the ultimate effect, we also simplify these two areas further into two independent areas as shown in Figure 8; we will still call

them areas I and II. The relationship between them is linked by the equivalence of the ultimate adiabatic flame temperatures in these two areas. We also assume that during the burning process the consumption ratios of the oxidation reagent and binder in these two areas are the same as the weight ratio of the oxidation reagent and binder in the propellant. So the total consumption rate of the propellant is :

$$m_t = \frac{\gamma}{\alpha} m_{ox_1} + \frac{(1-\gamma)}{\alpha} m_{ox_1} (S_{ox}/S_b) \quad (1)$$

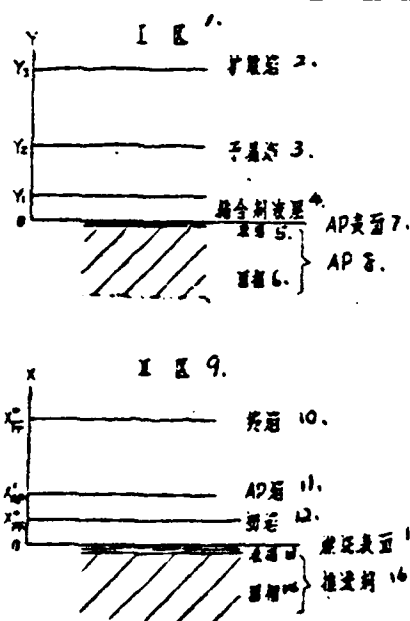


图 8 I、II 区的一维模型 17.

1. area I ; 2. diffused flame ; 3. pre-mixed flame
4. liquid binder layer ; 5. liquid phase ; 6. solid phase ;
7. AP surface ; 8. AP ; 9. area II ; 10. final flame ;
11. AP flame ; 12. initial flame ; 13. liquid phase ;
14. solid phase ; 15. burning surface ; 16. propellant ;
17. Figure 8 A one-dimensional model of areas I and II.

We will now treat areas I and II separately :

Area I : Based on the hypothesis that the condensed phase reaction exists and that the combustion speed is controlled by the condensed phase reaction with reverse-direction gasification, we can obtain the following equation according to reference [26]:

$$m_{ox} = \frac{1}{1-G} A_0' e^{-E_{ox}/(R \cdot T_s)} \left[ 1 - \frac{(P_s)_{AP(g)}}{P_{AP(g),s}(T_s)} \right] \quad (2)$$

For simplicity, here we have already applied the assumption Jacobs and Russell-Jones [25] proposed which treats  $NH_3(g)$  and  $HClO_4(g)$  as a single unified AP evaporation gas.  $P_{AP(g),s}(T_s)$  is the equilibrium evaporation pressure of AP under a temperature  $T_s$ . From the Clausius-Clapeyron equation we can obtain the approximated assumption :

$$P_{AP(g),s}(T_s) = B_1 \exp \left( \frac{-q}{R \cdot T_s} \right) \quad (3)$$

We can further deduce the following equation from the facts that the total pressure under the covering liquid layer equals the combustion pressure and that the mass concentration ratio of the condensed phase product and the AP vapor on the evaporation surface equals  $G/(1-G)$  :

$$(P_s)_{AP(g)} = \frac{P}{1 + \frac{G}{1-G} \frac{W_{AP(g)}}{W_c}} \quad (4)$$

Now we can obtain the continuity equation for area I

as :

$$m_{ox_1} = \frac{1}{1-G} A_1 \exp\left(-\frac{E_{ox_1}}{R^* T_s}\right) \left[ 1 - \frac{P_{exp}\left(\frac{q}{R^* T_s}\right)}{B_1 \left(1 + \frac{G}{1-G} \frac{W_{AP(g)}}{W_c}\right)} \right] \quad (5)$$

We can further set the origin of our one-dimensional coordinate system on the AP surface that is covered by the binder, as shown in Figure 8, and place the moving coordinate system which moves towards the interior at the combustion speed of the propellant  $r$ . We can then obtain the following equation when we assume that the thermodynamic parameter is a constant :

$$C_p \rho_r r \frac{dT}{dY} = \lambda \frac{dT}{dY} + \rho_r r [Q_s F_1(Y) - (1-\alpha) Q_r F_2(Y)] \quad (6)$$

In this equation  $F_1(Y)$ ,  $F_2(Y)$  are functions of the heat release; they describe individually the heat release conditions associated with the heat dissociation in the pre-mixed flame and on the surface of the binder. For simplicity, we assume that the heat releases are in pulses and they can be represented by  $\delta$  functions; we can then have :

$$\frac{dT}{dY} = \frac{1}{A} \frac{dT}{dY} + \frac{Q_s}{C_p} \delta(Y-Y_s) - (1-\alpha) \frac{Q_r}{C_p} \delta(Y-Y_r) \quad (7)$$

In this equation  $A = \frac{C_p \rho_r r}{\lambda}$ , the boundary conditions are :

$$\begin{cases} \text{when } Y=0, & T=T_s \\ \text{when } Y=Y_3, & T=T_f. \end{cases} \quad (8)$$

We can now seek solution of the equation by using the Lagrange transformation, and also take into consideration the relationship

of thermal equilibrium on the AP surface :

$$\lambda \frac{dT}{dy} \Big|_{y=0} = \rho_p r \{ a[(1-G)Q_s - GQ_L] + C_p(T_s - T_0) \} \quad (9)$$

We can then obtain a representative equation concerning  $T_s$  :

$$T_s = T_0 + a \frac{GQ_L - (1-G)Q_s}{C_p} - (1-a) \frac{Q_p}{C_p} \exp(-\xi_1^*) + \frac{Q_p}{C_p} \exp(-\xi_2^*) \\ + \left[ T_p - T_0 - a \frac{GQ_L - (1-G)Q_s}{C_p} + (1-a) \frac{Q_p}{C_p} - \frac{Q_p}{C_p} \right] \exp(-\xi_2^*) \quad (10)$$

Here  $\xi_1^* = \frac{C_p h m_{ox1}}{\lambda a}$  ; according to the assumption of the physical model we can set h as

$$h = \frac{B_2 \rho_p a}{(1-a) m_{ox1}} \quad (11)$$

$B_2$  is a parameter which primarily characterizes the mobility of the molten binder liquid (which possibly contains aluminum powder) and the structure of the burning surface. In this way,

$$\xi_1^* = \frac{C_p B_2 \rho_p}{\lambda (1-a)} \quad (12)$$

Since the pre-mixed flame and the diffused flame are separately determined by the chemical reaction speed and the chemical reaction as well as the diffusion speed, we then have :

$$\xi_2^* = \frac{C_p m_{ox1}}{K_1 \lambda a^2 P^{n_1}} + \xi_1^* \quad (13)$$

$$\xi_2^* = \frac{C_p m_{ox1}}{\lambda a^2} \left[ \frac{B_1 P d^2}{\rho_p D_1 T_1^{1.75}} + \frac{1}{K_1 P^{n_1}} \right] + \xi_1^* \quad (14)$$

Area II : By applying entirely similar steps as in area I, we have :

$$T_s = T_0 + \alpha \frac{GQ_s - (1-G)Q_s}{C_p} - (1-\alpha) \frac{Q_p}{C_p} + (1-\beta_p) \alpha \frac{Q_{AP}}{C_p} \exp(-\dot{\xi}_{AP}^*)$$

$$+ \beta_p \frac{Q_{PP}}{C_p} \exp(-\dot{\xi}_{PP}^*) + \left[ T_f - T_0 + (1-\alpha) \frac{Q_p}{C_p} - \alpha \frac{GQ_s - (1-G)Q_s}{C_p} \right.$$

$$\left. - (1-\beta_p) \alpha \frac{Q_{AP}}{C_p} - \beta_p \frac{Q_{PP}}{C_p} \right] \exp(-\dot{\xi}_{PP}^*) \quad (15)$$

Here  $\beta_p = \frac{A_{PH} X_{AP1}^* - X_{PR}^*}{K_{PD}^*}$  , (while  $X_{AP1}^* = m_{Ox_{11}} / (K_{AP} P^{*AP})$ ,  $X_{PP}^* =$  (A)

$$X_{PO}^* + X_{PR}^*, X_{PO}^* = \frac{B_{PP} m_{11} P d^2}{\rho_g D_s T_{PP}^{1/3}}, X_{PR}^* = \frac{m_{11}}{K_{PP} P^{*PP}})$$

$$\dot{\xi}_{AP}^* = \frac{C_p (S_{Ox}/S_0) \dot{m}_{Ox_{11}}}{\alpha K_{AP1} \lambda P^{*AP1}} \quad (16)$$

$$\dot{\xi}_{PP}^* = \frac{C_p (S_{Ox}/S_0) \dot{m}_{Ox_{11}}}{\lambda \alpha^2} \left[ \frac{B_{PP} P d^2}{\rho_g D_s T_{PP}^{1/3}} + \frac{1}{K_{PP} P^{*PP}} \right] \quad (17)$$

$$\dot{\xi}_{PR}^* = \frac{C_p (S_{Ox}/S_0) \dot{m}_{Ox_{11}}}{\lambda \alpha^2} \left[ \frac{B_{PP} P d^2}{\rho_g D_s T_{PP}^{1/3}} + \frac{1}{K_{AP1} P^{*AP1}} \right] \quad (18)$$

We also have  $S_{Ox}/S_0 = \frac{\zeta \left[ 6 \left( \frac{h}{d} \right)^2 + 1 \right]}{6 \zeta \left( \frac{h}{d} \right)^2 + 1}$  , while  $\frac{h}{d} = \frac{1}{2} \left( 1 \pm \frac{1}{\sqrt{3}} \right) \times$  (B)

$$(1 - m_{Ox_{11}} \rho_l / m_{11} \rho_{AP}) + \frac{m_{Ox_{11}} t_{120}}{\rho_{AP} d},$$

$$t_{120} = K_d d^{2/3} / P^{2/3}.$$

Similarly, we can obtain the continuity equations :

$$m_{Ox_{11}} = A_{Ox}^0 \exp \left( - \frac{E_{Ox}}{R^* T_s} \right) \quad (19)$$

$$m_{11} = A_1 \exp \left( - \frac{E_1}{R^* T_s} \right) \quad (20)$$



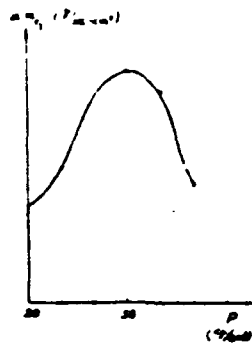
From the simultaneous equations above we can obviously obtain the relationship between the combustion rate on the entire surface and the pressure :  $F(\dot{m}_t, P) = 0$ .

## V DISCUSSION

Since there has been numerous available computational results and procedures concerning area II (such as references [27], [28]), we will only carry out the computations for area I here. The results of the computations based on the data sets in Table 2 are shown in Figure 9. When considering different combinations of different proportionalities in area II where the pressure exponents are always positive, we can obtain the conditions where the relationship between the mean combustion speed and the pressure will show positive, zero, and negative pressure exponents when the pressure exceeds a certain value. The mean combustion speed is estimated for the entire surface and the results are shown in Figure 10.

$A'_{ox}$	$1.848 \times 10^4 \text{ g/cm}^2 \text{ sec}$	$a$	0.8
$E_{ox}$	$22.0 \times 10^3 \text{ cal/mole}$	$C_p$	0.3 cal/g·°K
$B_1$	$3.48 \times 10^5$	$\lambda$	$0.3 \times 10^{-2}$ cal/cm·sec·°K
$B_2$	$0.79 \times 10^{-4}$	$Q_L$	111.0 cal/g
$B_3$	1.0	$Q_S$	120.9 cal/g
$q$	$20.8 \times 10^3 \text{ cal/mole}$	$Q_F$	50.0 cal/g
$G$	$0.0 (P=70 \text{ kg/cm}^2)$	$Q_D$	605.0 cal/g
	$0.3 (P=20, 30, 60 \text{ kg/cm}^2)$	$\rho_l$	1.05 g/cm <sup>3</sup>
	$0 (P=50 \text{ kg/cm}^2)$	$K_1$	1.12 g/cm <sup>3</sup> ·sec·atm <sup>1.5</sup>
$W_o$	28.4 g/mole	$K_2$	30.0 g/cm <sup>3</sup> ·sec·atm <sup>1.5</sup>
$W_{A, P(1)}$	117.5 g/mole	$n_1$	1.8
$W_s$	26.2 g/mole	$n_2$	1.5
$T_i$	2900 °K	$d$	180.0 $\mu$
$T_s$	300 °K	$D_s$	$5.97 \times 10^{-4} \text{ cm}^2/\text{sec}$
$T_o$	2150 °K		

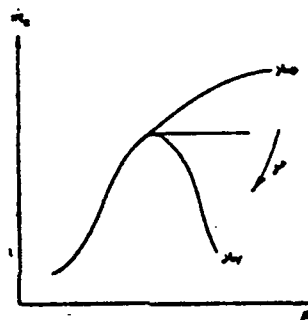
1. Table 2 The original data sets used for the area I computations



1. 图9 I区质量燃烧速度与压力的关系

1. Figure 9 The relationship between mass combustion speed and pressure in area I.

---



1. 图10 全表面平均速度与压力之间可能出现的多种关系

1. Figure 10 The multiple kinds of relationships that can exist between the mean combustion speed estimated over the entire surface and the pressure.

---

In this way, we can first try to explain the already discovered phenomena more reasonably :

1. Under the condition that the AP surface is covered with a layer of the melten binder liquid, the pressure exponents may not have to be either zero or negative. They can actually

be positive. This is why that we should not be surprised to find the existence of this covering phenomenon associated with prescriptions with positive pressure exponents. This is what can and should be considered in a theoretical model.

2. The covering phenomena are also obvious and widespread under low pressures for non "mesa" areas or areas neighboring the "mesa" areas. This also does not contradict our model. This is the case since the pressure exponents in area I are also positive under low pressures so in this sense they are the same as those in area II. In other words, the increase in the fractional covered area  $\gamma$  will not change the pressure exponents to zero or negative values under low pressures.

In sum, the fact that the covering of the melten binder liquid on top of the AP surface is not a particular phenomenon of the propellant in the "mesa" area can be explained reasonably.

3. By replacing the local extinction under the area where the AP is covered by the melten binder with the abnormal burning, we can provide a more reasonable explanation for the existence of the self-excited vibration under the pressure condition associated with extensive covering.

Secondly, we can see that this model can fully explain the phenomena that the AP composite propellant can exhibit positive, zero, and negative pressure exponents. Furthermore,

when  $r=0$  our model reduces back to the "BDP" type model which applies only for propellant with a binder that is difficult to melt. This shows that our model can be used for a much wider range of applications.

At the same time, we can see from the mathematical treatment mentioned above that through the computations we can not only explain the dependency relationship between the combustion speed and the pressure, but we can also calculate the influence of the initial temperature on the combustion speed based on the influence of the initial temperature on the surface temperature. We can then calculate the temperature sensitivity coefficient associated with the combustion speed. In the meantime, we can also see from the inclusion of the diameter of the oxidation reagent particle in  $\xi^*$  ( $r$  also includes the relationship with it) that we can make theoretical predictions about the effects of the diameter of the oxidation reagent particle on the combustion speed, temperature sensitivity coefficient, and the pressure exponents.

In addition, similar to the basic "BDP" and "GDF" models, this model can be further developed into a statistical model which can take into consideration the effect of the size distribution of the AP particles. This model can also serve as a basis for the study of the erosive burning and un-steady burning of the propellants which include the ones with negative

pressure exponents, just like the way the advocates of the "PEM" model are doing it<sup>[27]</sup>.

Of course the types of propellants involved in this study are limited and the model has not yet given the quantitative relationship between the fractional covering area  $\gamma$  and the reaction fraction  $G$ , as well as the factors that are affecting them. This is why further study and perfection of the model are necessary.

## VI CONCLUSION

1. Through SEM and photography through the transparent window of the combustion chamber we discovered : the covering of the molten binder on the surface of the AP crystal under certain conditions is not a particular phenomenon of the PU propellant in the "mesa" area; rather it is a general phenomenon that can take place over a much extensive area. In addition, this kind of covering may not result in local extinction.

2. We think that the cause of the "plateau" and "mesa" effects of the composite propellants with easily melting binders is not local extinction; rather it is the abnormal burning of propellant with condensed phase reaction and reverse-direction gasification associated with different covering conditions of

the AP by the molten binder liquid layer.

3. Since there is widespread existence of the covering of the surface of the oxidation reagent by the molten binder, the assumptions of the "GDF" and "BDP" models are destroyed. This is why we need a new basic model which can address the problem fully. The model proposed by this paper has the potential of becoming a basis for the development of such a new model.

4. The model proposed by this paper not only exhibits the superior points of being able to explain fully the "plateau", "mesa", and normal burning behavior, but it is also capable of explaining the effects of initial temperature and the AP particle size on the burning characteristics. The latter is similar to the capability of the traditional models such as the "GDF" and "BDP". At the same time, our model can also serve as a basis for the study of the erosive burning and un-steady burning of the propellants which include those with negative pressure exponents.

5. The model proposed by this paper needs to be further perfected.

#### REFERENCES

- [1] He Guo Zhong, Yang Pei Qing, A multi-layer flame model for the study of the combustion speed of the solid and solid-liquid propellants, A compilation of the

papers presented at the meeting of the combustion and erosive burning of rocket propellers, Compiled by the Institute of Physical Chemistry, Academia Sinica, p. 255.

- [3] Xu Wen Gan, An examination into the concept of impulse power adjustment for the solid rocket propeller, Journal of Astronautics, Volume 1, 1981.
- [16] Wudai Shiwen, Tengyuan, Mian · Qingshui Shengsheng, Zhongcun Lichun · Yiteng Kemi, The relationship between rapid decrease in pressure and interrupted combustion for the interrupted impulse power type solid rocket propeller, NAL TR-461.
- [21] D.M. Watt and E.E. Petersen, Deflagration and Deflagration Limits of Single Crystals of AP, AF-AFOSR 959-65 Dec. 1968, quote from [20] .
- [26] P.A. Williams, Combustion Theory, Addison-Wesley, Reading, Mass, 1965 (see translated version in Chinese, translated by Li Yin Ting and Jia Wen Kui, published in 1976).

- [1] 何国钟、梅培青, 用于固体和液体推进剂燃烧研究的多层火焰模型, 火箭发动机的燃烧与烧蚀会议论文集, 中国科学院化学研究所编 p. 255.
- [2] J. H. Robert, The Prediction of the burning Rate Exponent of Solid Propellants, AD-815882, Dec., 1966.
- [3] 徐温干, 固体火箭发动机推力调节方案探讨, 宇航学报 1981年 第1期
- [4] J. Cohen, L. C. Landers and R.L. Lou, Zero Time Delay Controllable Solid Propellant Gas Generators, Paper. AIAA 76-691.
- [5] D. B. Spalding, The Theory of Burning of Solid and Liquid Propellants, J. Combustion and Flame, Vol. 4, No. 1 (1960).
- [6] E. K. Bastress, Modification of the Burning Rates of Ammonium Perchlorate Solid Propellants by Particle Size Control, Ph. D. Thesis, Department of Aeronautical Engineering, Princeton University.
- [7] M. Barrère and L. Nadand, Les Domaines de Combustion des Poudres Composites, La Recherche Aéronautique No. 98, pp. 15-29, 1964.
- [8] J. A. Steinz, P. L. Stang and M. Summerfield, The Burning Mechanism of Ammonium Perchlorate Based Composite Solid Propellants, Paper. AIAA 68-658, AD-683944.
- [9] Chaihan, Burning Mechanism of Ammonium Perchlorate Propellants, Solid Propellant Rocket

- Research, Vol. 1 of progress in Astronautics and Rocketry, PP.227-242, 1960.
- [10] R. L. Derr and T. L. Boggs, Role of SEM in the Study of Solid Propellant Combustion Part III, AD-726293.
  - [11] W. G. Schmidt, The Effect of Solid Phase Reaction on the Ballistic Properties of Propellants, NASA CR-66457 May, 1969.
  - [12] T. Godai, et al., Pressure Exponent of Controllable Solid Rocket Propellants, Paper. AIAA 72-1135.
  - [13] J. Cohen, L. C. Landers and R. L. Lou, Zero Time Delay Controllable Solid Propellant Gas Generators, J. Spacecrafts and Rockets, May 1977.
  - [14] C. Guirao and F. A. Williams, A model for Ammonium Perchlorate Deflagration between 20 and 100 atm, J. AIAA Vol. 9, No. 7, 1971.
  - [15] C. L. Merkle, et al, Extinguishment of Solid Propellants by Rapid Depressurization, AD-697661.
  - [16] 五光寛文、藤原、勉・清水盛生、神村利春・伊藤克弥、推力半断型固体ロケット用プロペラント急圧急減圧燃焼中の注目の関係、NAL TR-461.
  - [17] W. C. Strahle, J. C. Handley and N. Kumar, Catalytic Behavior in Solid Propellant, AD-770601 (1973).
  - [18] J. C. Handley, E. W. Price and A. Ghosh, Combustion of Non-Aluminized Binders in Tapered Sandwiches, AD-A084681, pp. 127-147 (1979).
  - [19] N. Cohen, Combustion Response Modeling for Composite Solid Propellants, JPL/AFRPL-76-F.
  - [20] T. L. Boggs, Deflagration Rate, Surface Structure and Subsurface Profile of self-Deflagrating Single Crystals of AP, J. AIAA Vol. 8, No. 5, 1970, AD-726234.
  - [21] D. M. Watt and E. E. Petersen, Deflagration and Deflagration Limits of single Crystals of AP, AF-AFOSR 959-65 Dec. 1968, 特引用 [20].
  - [22] Raymond Friedman, et al, Deflagration of Ammonium Perchlorate, 6 Symposium on Combustion, 1957.
  - [23] C. Guirao and F. A. Williams, Sublimation of AP, J. Physical Chemistry Vol. 73 No. 12, PP. 4302-4311 (1969).
  - [24] P. W. M. Jacobs and A. Russell-Jones, On the Mechanism of the Decomposition of Ammonium Perchlorate, AIAA J. Vol. 5, No. 4, P. 829-, (1967).
  - [25] P. W. M. Jacobs and A. Russell-Jones, Sublimation of Ammonium Perchlorate, J. Physical Chemistry Vol. 72, No. 1, P. 202-, 1968.
  - [26] F. A. Williams, Combustion Theory, Addison-Wesley, Reading, Mass, 1965 (見中譯本, 1973 年平賀孝、夏文彦譯 1976 年印刷).
  - [27] J. A. Condon and J. R. Osborn, The Effect of Oxidized Particle Size Distribution on the Steady and Nonsteady Combustion of Composite Propellants, AD-A056892.
  - [28] AFOSR, Multiple-Flame Combustion Model Fortran IV Computer Program, AD-781128.